Effect of Phosphorylation on the Interdomain Interaction of the Response Regulator, NarL†

Aimee M. Eldridge,‡ Hyun-Seo Kang,‡ Eric Johnson,§ Robert Gunsalus,§ and Frederick W. Dahlquist*,‡

Institute of Molecular Biology, University of Oregon, Eugene, Oregon 97403, and Department of Microbiology, Immunology, and Molecular Genetics, University of California, Los Angeles, California 90095-1489

Received June 6, 2002; Revised Manuscript Received October 16, 2002

ABSTRACT: DNA binding by the effector domain (NarLC) of the response regulator, NarL, is modulated by the phosphorylation state of the receiver domain (NarLN). The receiver domain appears to block the site of DNA binding in the nonphosphorylated state. Phosphorylation is proposed to disrupt this interaction, causing the effector domain to be released and free to bind DNA (Baikalov, I., Schroder, I., Kaczor-Grzeskowiak, M., Grzeskowiak, K., Gunsalus, R. P., and Dickerson, R. E. (1996) *Biochemistry 35*, 11053−61). To better understand this modulation, we analyzed the interaction between the two domains in the absence of a polypeptide linkage. Using multidimensional NMR, we mapped chemical shift changes that occurred during a titration between the two isolated domains. Specific residues in NarLC exhibit large chemical shift changes upon the addition of NarLN. These residues are primarily at the interface between the two domains as seen in the crystal structure. Using the residues with the largest chemical shift changes, we observed a dissociation constant of 88 ± 7 μM. In the presence of 10 mM $MgCl_2$, the affinity is reduced 4-fold to about 350 μM. This work shows that the domains interact in trans and that this interaction, while fairly weak, provides a way to monitor the energetics of domain−domain interaction in this system. Phosphorylation of NarLN by a small-molecule phosphate donor, phosphoramidate, decreases this interaction about 25-fold from the nonphosphorylated sample. The results support the model that the mechanism of activation of NarL involves a disruption of the interdomain interface and suggests that the linker is not necessary for the transmission of signal across the domain interface. The linker does play a role in increasing the local concentration of the domains and therefore increasing the amount of closed conformation with respect to the open conformation. We estimate the levels of open conformation to be low (about 1%) in the nonphosphorylated state in the absence of magnesium ion and much higher in the phospho state (near 50%). This modulation of the open or active state via the interaction at the interface may also be applicable to other multidomain response regulator proteins.

Escherichia coli employs a two-component signaling system to regulate the nitrate- and nitrite-dependent expression of anaerobic respiratory genes (for reviews, see refs *2* and *3*). This signaling system is analogous to the large family of bacterial two-component signal transduction systems that elicit an output function such as regulation of gene expression or of motility in response to environmental cues (see recent reviews in refs *4*−*6*). These systems are generally characterized as having a sensory-transmitter component and a response regulator component. The sensory-transmitter protein is a histidine kinase that autophosphorylates upon detection of changes in the environment. The signal is transferred to the response regulator via phosphorylation of an aspartic acid residue on the conserved regulatory domain. In general, phosphorylation activates the response regulator through an attached effector domain.

The nitrate-, nitrite-sensing system is comprised of two histidine kinases, NarX and NarQ, and two response regulators, NarL and NarP. The purpose of the duplication is still unclear, but the proteins behave in an overlapping but nonidentical manner (for a review, see ref *7*). As described above, the kinases autophosphorylate in response to nitrate and nitrite in the environment and transfer this phosphate to NarL and NarP. Once phosphorylated, NarL and NarP activate and repress transcription of a variety of anaerobic respiration genes. Much work has been done on response regulators to understand the structural basis for phosphorylation-dependent regulation of an output function (see recent reviews in refs *4* and *5*). One of the first structures of a complete response regulator was of NarL (*1*), shown in Figure 1.

As is seen in many other response regulators, NarL is comprised of two domains, an amino-terminal receiver domain (NarLN) and a carboxy-terminal effector domain (NarLC). NarLN is a five-stranded β-sheet surrounded by five α-helices having high structural homology to the chemotaxis response regulator protein, CheY. In Figure 1, NarLN is below NarLC with the site of phosphorylation, Asp-59 (*10*), depicted as a red sphere. NarLC is a four-helix bundle in which the two middle helices adopt a helix−turn−helix (HTH) DNA-binding motif. The receiver domain

† This work was supported by grants from the National Institutes of Health AI21678 (R.G.) and GM57766 (F.W.D.).

* Author to whom correspondence should be addressed. E-mail: fwd@nmr.uoregon.edu.

‡ University of Oregon.

§ University of California.

10.1021/bi026254+ CCC: $22.00
Published on Web 11/23/2002

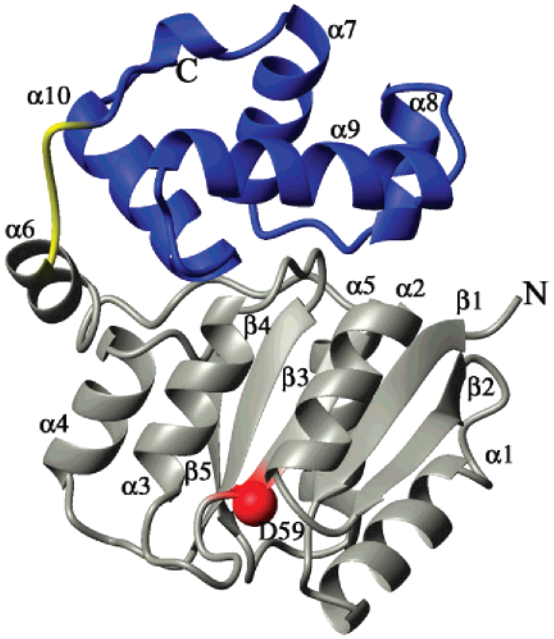

FIGURE 1: Ribbon diagram of the X-ray crystal structure of NarL using coordinates from the Brookhaven Protein Database 1a04 (*8*). The C-terminal DNA binding domain is blue and located above the N-terminal domain. The N-terminal regulatory domain is represented in light gray with the site of phosphorylation, Asp-59, depicted as a red sphere. The region containing the seven residue disordered tether is shown in yellow. The figure was created with MolMol (*9*).

contains an additional helix, which in conjunction with a disordered tether forms the polypeptide linkage between the two domains. Thirteen residues in the tether are not visible in the original structure. However, five additional residues are visible in a later structure of NarL (*8*). The orientation of the domains with respect to each other is the same throughout the structures. In addition, there are only seven residues missing in the later crystal structure making an alternative pairing of domains unlikely.

Modeling B-DNA into the HTH motif of the C-terminal domain in a manner consistent with other HTH DNA-binding proteins led the authors to propose a DNA-binding interface and putative DNA-binding residues. However, the proposed DNA-binding interface overlaps with the interdomain interface in the unphosphorylated structure. Therefore, DNA binding to NarLC would be blocked by the presence of NarLN. It is proposed that phosphorylation relieves this inhibition by disrupting the interdomain interface, allowing access to the DNA binding site (*1*). The direct regulation of the effector domain by the receiver domain has been observed in other response regulators, most notably the methylesterase from chemotaxis, CheB (*11*, *12*). In CheB, the unphosphorylated receiver domain appears to inhibit the activity of the methylesterase domain by blocking access to the catalytic triad. In both of these cases, the interaction between the domains is thought to be relatively weak so that this blocking can be reversed by phosphorylation. In addition, there is speculation that the polypeptide tether is required for the interaction between the two domains (*5*).

To measure the energetics of the interaction between the domains, we removed the polypeptide linker between them and produced two unlinked domains. We could then directly measure the interaction between them by measuring their binding affinities. Next, we measured the change in affinity between the unlinked domains when NarLN was phosphorylated. To define the interaction interface, we used multidimensional NMR to follow the changes in chemical shift of specific residues in the effector domain upon the addition of the receiver domain. This putative binding interface was mapped onto the structure and is consistent with the interface seen in the crystal structures. The binding affinity is relatively weak and was further decreased by the addition of a small molecule phosphate donor. These results indicate a direct role for the interdomain interaction in the phosphorylation-dependent modulation of the active state of NarL and a modulation of this interaction by a factor of 100 or so by phosphorylation.

MATERIALS AND METHODS

Expression and Purification of Protein Samples. The NarLC gene encoding for residues 145−216 was cloned into the pET3a vector (Novagen). The resulting vector was named pIS78 vector and contains a T7 IPTG-inducible promoter. For protein overexpression, the plasmid was transformed into the strain BL21λDE3. Protein labeled uniformly with ^{15}N and ^{13}C was made by growing the cells in minimal media containing $^{15}NH_4Cl$ (Isotec) and ^{13}C-labeled glucose (Isotec) as the only nitrogen and carbon sources. Cells were grown at 37 °C with shaking to an optical density at 600 nm (OD_{600}) of 1.0. Protein production was induced by the addition of 0.5 mM isopropyl-β-D-thiogalactopyranoside (IPTG), and the cells were allowed to grow for 4 or more h. The cells were harvested by centrifugation at 5000 rpm for 30 min at 4 °C. Cell pellets were resuspended in 50 mM 3-(*N*-morpholino)propanesulfonic acid (MOPS), 50 mM potassium chloride (KCl), and 1 mM phenylmethylsulfonyl fluoride (PMSF) at pH 6.8 and broken by passage through a French press at least three times at 20 000 psi. The lysate was centrifuged at 4 °C for 40 min at 14 000 rpm, and the supernatant was dialyzed overnight against the original buffer. A CM-Sepharose CL-6B cation-exchange column (Sigma) was prepared by washing with 50 mM MOPS and 50 mM KCl buffer at pH 6.8. Once the column was equilibrated, the dialyzed sample was loaded via gravity onto the column. After being loaded, the column was washed with >3 column volumes of the original wash buffer. The protein was eluted with a salt gradient of 50 mM−1 M KCl in 50 mM MOPS at pH 6.8. Fractions containing only the C-terminal domain, as assessed by SDS−PAGE, were pooled and then dialyzed against 50 mM potassium phosphate and 50 mM KCl at pH 6.8. The protein was concentrated first by using a Centriprep (Amicon) and then a Microsep microconcentrator (Pall Filtron) both with a molecular weight cutoff of 3000 kDa. The single-labeled (^{15}N) sample used in the titration experiments was grown, purified, and concentrated in the same manner as the double-label sample.

The gene encoding for residues 1−140 of NarLN was cloned into the pQE9 vector (Qiagen) and transformed into the strain JM109. Unlabeled NarLN protein was produced by growth in LBH media at 37 °C with shaking. The cells were induced at an OD_{600} of 0.5 with 1 mM IPTG. After 4 or more h, the cells were harvested by centrifugation at 5000 rpm for 30 min at 4 °C. Purification of NarLN took advantage of an N-terminal his-tag. The cells were resus-

pended in 50 mM potassium phosphate, 50 mM KCl, and 1 mM PMSF at pH 7.6. The cells were broken by passage through a French press at least three times at 20 000 psi. Cell debris was removed by centrifugation at 14 000 rpm for 45 min at 4 °C. The supernatant was loaded onto a Ni−NTA Agarose column (Qiagen) that was preequilibrated with 50 mM potassium phosphate, 50 mM KCl, and 5 mM imidazole at pH 7.6. The column was washed with the equilibration buffer. To remove nontagged proteins from the column, the column was washed with high-salt, 50 mM potassium phosphate, and 1 M KCl at pH 7.6, then followed by another wash with the equilibration buffer. Next, the column was washed with buffer containing 20 mM imidazole and then by buffer containing 50 mM imidazole. The protein was eluted from the column with 100 mM imidazole in 50 mM potassium phosphate and 50 mM KCl at pH 7.6. Fractions containing only pure N-terminal domain were pooled and dialyzed overnight against 50 mM potassium phosphate and 50 mM KCl at pH 6.8. The protein was concentrated to 2.5 mM. Concentrations of the proteins were determined by amino acid composition analysis from an acid hydrolysis reaction (AAA Service Laboratory) and by BCA assay.

General NMR. A Varian INOVA 600 MHz spectrometer with a ^{1}H [$^{15}N/^{13}C$] 5-mm triple-resonance probe was used to obtain the NarLC assignment data. For the titration, the series of two-dimensional $^{1}H-^{15}N$ HSQC (*13*) spectra were recorded on a Varian UNITY 500 MHz spectrometer. All spectra were recorded at 25 °C. In addition, for all spectra the proton carrier frequency was set to water, and the ^{15}N carrier was set to 119 ppm. All NMR data were processed and analyzed with the program FELIX98 (Biosym).

Assignments. The $^{13}C,^{15}N$ sample of NarLC contained 0.7 mM protein in 50 mM potassium phosphate and 50 mM KCl at pH 6.8 with 10% $^{2}H_2O$ and 0.02% sodium azide. To determine the assignments of peaks not visible at pH 6.8, additional spectra were also taken at pH 5.7 in the same buffer conditions. The sequential backbone resonance assignments were determined using the following gradient-enhanced triple resonance experiments: HNCACB (*14*), CBCA(CO)NH (*15*), and C(CO)NH (*16*).

Titration. The two proteins were dialyzed into the same buffer of 50 mM potassium phosphate and 50 mM KCl at pH 6.8. Each protein was subsequently diluted with the same buffer for the titration. In addition, $^{2}H_2O$ and sodium azide were added to the NMR samples to final concentrations of 10 and 0.02%, respectively. Throughout the titration the ^{15}N-NarLC concentration was held constant at 0.115 mM while the concentration of unlabeled NarLN was increased from 0 to 2.02 mM. After each step in the titration, a HSQC was recorded, and the peaks were analyzed for changes in chemical shift. Binding curves were analyzed in the manner of Kim et al. for one-to-one binding of ligand to a protein where the interaction is in fast exchange (*17*). The formula, fit by optimizing K_d and $\delta_b - \delta_f$ and performing a nonlinear least-squares analysis, is as follows:

$$\Delta\delta_{obs} = \frac{\delta_b - \delta_f}{2C_o}\left(N_o + C_o + K_d - \sqrt{(N_o + C_o + K_d)^2 - 4N_oC_o}\right) \quad (1)$$

where C_o is the total concentration of NarLC (0.115 mM), N_o is the total concentration of NarLN (0−2.02 mM), $\Delta\delta_{obs}$ is the observed chemical shift, and $\delta_b - \delta_f$ is the total chemical shift difference from the bound to the unbound state. Binding curves and dissociation constants were calculated for the residues with the largest total chemical shift difference: 153, 164, 168, 169, 170, 171, 174, 175, 176, 183, 189, 192, 195, 200, 201, 202, 204, 207, 209, 211, and 212. The program KaleidaGraph (Synergy Software) was used to perform the nonlinear least-squares fit to the data.

Phosphorylation. To assess the effect of phosphorylation on the interaction, 120 mM phosphoramidate and 10 mM $MgCl_2$ were added to the final sample, and a 2-h HSQC was recorded. For direct comparison, a sample of 0.115 mM ^{15}N-NarLC was also treated in this manner. Also, to assess the ability of phosphoramidate to phosphorylate NarLN, a 1.4 mM ^{15}N-NarLN sample was treated with 120 mM phosphoramidate and 10 mM $MgCl_2$ with HSQC spectra recorded every 20 min for 12 h. The spectrum of ^{15}N-NarLN was significantly altered in the first 20-min time point after the addition of phosphoramidate; these changes were constant in all subsequent spectra up to and beyond 12 h. These spectral changes are the same (data not shown) as the spectral changes seen with a known small-molecule phosphodonor to NarL, acetyl phosphate (data not shown) (*18*). In addition, freshly isolated NarLN is phosphorylated as judged by its HSQC spectrum. The spectrum converts to that of the unphosphorylated state as the sample ages over several days. In both cases, there are only two spectra present as the protein spontaneously dephosphorylates, demonstrating a single site of phosphorylation. That site is most likely Asp59. Taken together, these results indicate that NarLN is phosphorylated by phosphoramidate, and the changes brought about by phosphorylation occur in much less than 20 min.

Calculation of the K_d under phosphorylation conditions was performed by combining the equations for K_d and for the fraction of NarLC bound:

$$\text{(a) } K_d = \frac{[C][N]}{[CN]} \text{ and (b) } f_{cbound} = \frac{[CN]}{[C] + [CN]} = \frac{\Delta\delta_{obs}}{\Delta\delta_{tot}} \quad (2)$$

to give

$$f_{cbound} = \frac{[N]}{[N] + K_d} = \frac{\Delta\delta_{obs}}{\Delta\delta_{tot}} \quad (3)$$

Assuming that $[N]$ is roughly equivalent to $[N_o]$, eq 3 can be solved for K_d using the total concentration of NarLN and the ratio of observed chemical shifts under phosphorylation conditions divided by the total change in chemical shift ($\Delta\delta_b - \Delta\delta_f$) from eq 1. The average ratio was calculated using the same residues as were used in the calculation of the dissociation constants (see above).

Local Concentration. The effective concentration was estimated by modeling the flexible linker as a wormlike chain using the persistence and contour lengths of the polypeptide chain and the end-to-end distance from first residue in the linker to the last residue in the linker as seen in the crystal structure (*19*). The following equation from Zhou was used to calculate the local concentration (*19*):

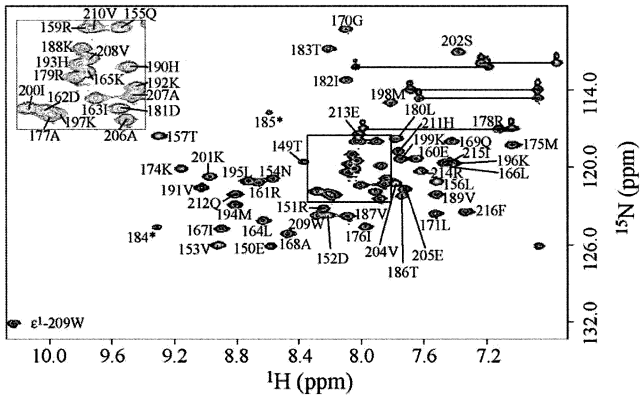

FIGURE 2: $^{15}N-^{1}H$ correlation spectrum of ^{15}N-labeled NarLC with residue assignments located next to the appropriate peak. The central region enclosed by the square is expanded and represented as an inset in the upper left corner of the spectrum. Starred residues (*) indicate residues with tentative assignments (see text).

$$p(d_0) = \left(\frac{3}{4\pi l_p l_c}\right)^{3/2} \exp\left(-\frac{3{d_0}^2}{4 l_p l_c}\right)\left(1 - \frac{5 l_p}{4 l_c} + \frac{2{d_0}^2}{{l_c}^2} - \frac{33{d_0}^4}{80 l_p {l_c}^3} - \frac{79{l_p}^2}{160{l_c}^2} - \frac{329{d_0}^2 l_p}{120{l_c}^3} + \frac{6799{d_0}^4}{1600{l_c}^4} - \frac{3441{d_0}^6}{2800 l_p {l_c}^5} + \frac{1089{d_0}^8}{12800{l_p}^2{l_c}^6}\right) \quad (5)$$

where d_0 is the end-to-end distance of the linker in the crystal structure and l_c and l_p are the contour and persistence lengths of the polypeptide linker, respectively. Values given in ref *19* were used in these calculations, $l_p = 3$ Å and $l_c = bL$, where b is the nearest $C_\alpha - C_\alpha$ distance (3.8 Å) and L is the number of residues in the linker. For NarL, the linker length was chosen to be 13 or 7 residues, the lengths of the disordered region in the first and second crystal structures, respectively. The corresponding end-to-end distance, d_0, for these linker lengths is 19.2 and 10 Å.

RESULTS

Backbone Resonance Assignments. The NarLC backbone resonance assignments ($^{1}H_N$, ^{15}N, and $^{13}C_\alpha$) and $^{13}C_\beta$ were determined for the majority of residues (Figure 2). Residues at the extreme N-terminus (before residue 149) and two other residues, 173 and 203, are unobservable in the $^{1}H-^{15}N$ HSQC at pH 6.8 and therefore could not be assigned. Also, residues 184 and 185 can only be tentatively assigned because of missing peaks in the HNCACB spectrum. Residue 184 has a fairly clear set of ($i - 1$) peaks in the CBCA-(CO)NH that are at the same chemical shifts as the C_α and C_β peaks of residue 183. Residue 185 has a C_α peak that is at the same chemical shift as an ($i - 1$) peak of residue 186 but has no C_β peak.

Titration. The amide assignments were used to follow the chemical shift changes that occurred upon titration with NarLN. Changes in the NarLC spectrum were observable at the lowest concentration of NarLN (~14 μM). Because of exchange broadening during the titration, several residues disappeared during the titration including 208V and 205E, and their final bound positions could not be determined unambiguously. However, the majority of residues affected

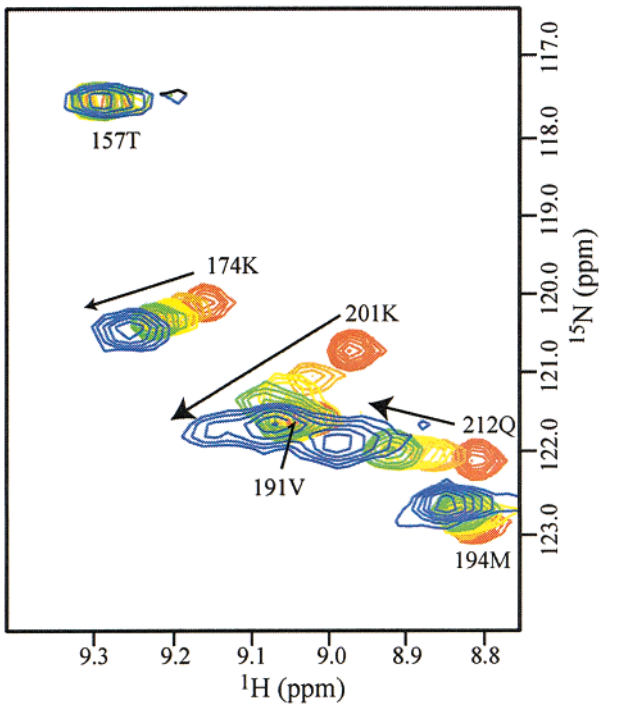

FIGURE 3: Section of the NarLC spectrum showing the change in chemical shift for particular residues as the concentration of NarLN increases. The arrows show the direction of the change in chemical shift with increasing concentrations of NarLN (0−2.02 mM).

by the addition of the regulatory domain could be tracked throughout the titration (Figure 3). The absolute value of the difference between the bound and the unbound proton and nitrogen chemical shifts is shown in the top two panels of Figure 4. The total chemical shift difference seen in the lower panel of the figure is the square root of the sum of the squared differences of the proton and nitrogen chemical shifts between the unbound to the bound state calculated in Hertz using the following equation:

$$\Delta\delta_{tot} = \sqrt{(\delta^{1}H)^2 + (\delta^{15}N)^2} \quad (4)$$

Residues in NarLC with large chemical shift differences upon the addition of the NarLN occur throughout the primary sequence of the molecule (Figure 4). However, when residues with changes greater than 50 Hertz are mapped onto the crystal structure, a putative binding interface emerges (Figure 5). Figure 5 is a ribbon diagram of NarL in the same orientation as Figure 1 with NarLN depicted in gray. The titration-induced chemical shift changes are mapped to the structure of NarLC with a ramp from blue to red over the range of 0 to >70 Hz. Residues in white have no data, either because they have no amide chemical shift assignments (prolines and unassigned residues), or because they are in regions with significant overlap. The residues with the largest chemical shift changes form an interface that is consistent with the interdomain interface determined by the crystal structure. These residues showed no discernible chemical shift changes upon addition of a different response regulator, CheY (data not shown), suggesting a specific interaction between the domains.

Dissociation constants were determined by analyzing the observed chemical shift of NarLC as a function of the concentration of NarLN (Figure 6). The K_d values were

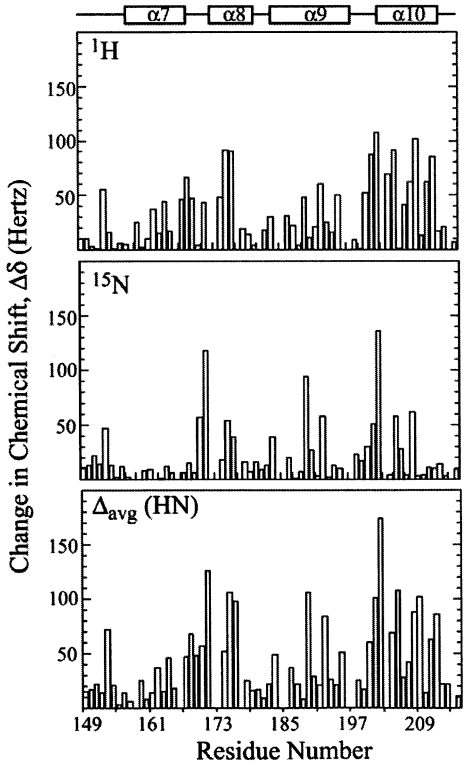

FIGURE 4: Chemical shift changes as a function of residue number for the unbound to the fully bound states. The top two panels contain the shift information for proton and nitrogen assessed separately, and the bottom panel contains the total chemical shift change (see eq 4). Secondary structure elements are shown at the top of the graphs.

extracted using eq 1 by adjusting the K_d and $\delta_b - \delta_f$ values during a least-squares fit to the titration data. The average K_d over all residues with changes over 50 Hz (see Materials and Methods) is 88 ± 7 μM. This affinity decreases about 4-fold in the presence of 10 mM magnesium chloride (data not shown), but the bound shifts change little.

Phosphorylation. Addition of 120 mM phosphoramidate and 10 mM $MgCl_2$ to the fully bound sample results in phosphorylation of NarLN and weakens the interaction between the domains. A decrease in binding is evident from the near return of the NarLC peaks to their unbound positions (Figure 7). The chemical shifts of the peaks in the phosphorylated sample were directly compared to a sample of the C-terminal domain treated in the same manner (120 mM phosphoramidate and 10 mM $MgCl_2$), and no shifts were observed. The observed chemical shift difference of the phosphorylated sample from unbound NarLC was very small as compared to the difference between the fully bound and the unbound NarLC (Figure 8). We can only estimate the change in affinity since we cannot saturate the complex when NarLN is phosphorylated. This clearly demonstrates a dramatic lowering of the affinity as a result of phosphorylation. If we assume that the average shift magnitude of the NarLC residues is about the same when bound to either the phosphorylated or the nonphosphorylated forms of NarLN, eq 3 can be used to estimate the dissociation constant for the complex when NarLN is phosphorylated. The value is about 12 mM or about 100-fold weaker than in the absence of phosphorylation and magnesium ion. This estimate is likely to correct within a factor of 2 or so.

The assumption of little change in the average chemical shift magnitude of NarLC when bound to phosphorylated NarLN is reasonable and is supported by the observed data, but we cannot prove it. The residues that show the largest shift in the unphosphorylated complex also have the largest shifts in the phosphorylated complex. Even if the exact values change, when they are averaged over the several residues that show shifts, these changes will likely be averaged to a small value.

Local Concentration. The binding interaction of the two domains increases significantly upon tethering with a flexible linker such as in the full-length NarL. The effective or local concentration of the domains varies inversely to the linker length. Using the method of Zhou (*19*) (see Materials and Methods), the local concentration for NarL was calculated to be 20 mM using a linker length of 13 residues and 110

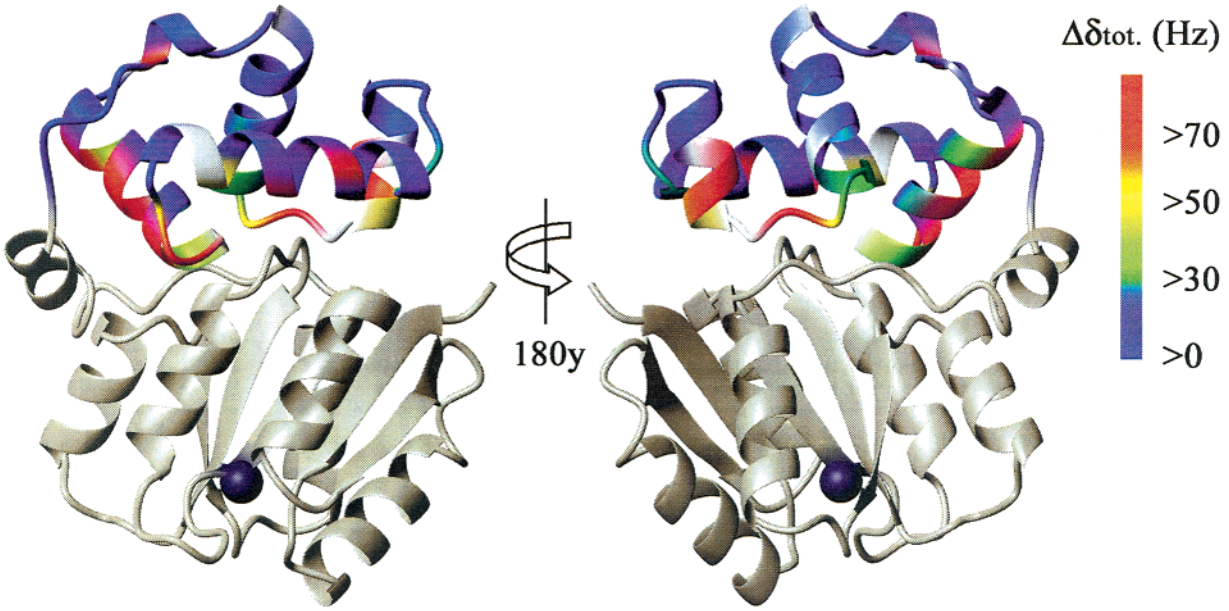

FIGURE 5: Ribbon diagram of NarL in the same orientation as in Figure 1 (left) and with a 180° rotation along the vertical axis (right). The NarL structure is colored in a ramp from blue to red representing the changes in chemical shift in NarLC upon the addition of NarLN. Residues in white are unassigned or are in regions with significant overlap.

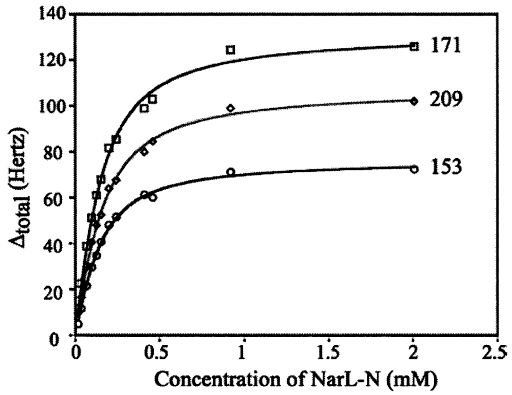

FIGURE 6: Total change in chemical shift as a function of NarLN concentration for three representative residues in NarLC. The concentration of NarLC was held constant at 114.5 μM throughout the titration. The calculated binding curves are shown for residues 171, 209, and 153 with dissociation constants of 87, 97, and 83 μM, respectively.

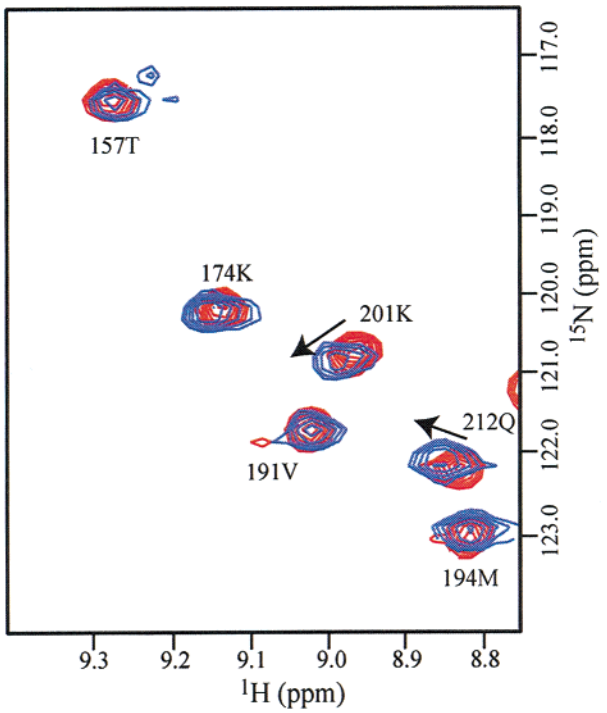

FIGURE 7: Section of the NarLC spectrum showing chemical shifts in the presence of 120 mM phosphoramidate and 10 mM $MgCl_2$. In red is NarLC alone, and in blue is NarLC with 2.02 mM NarLN.

mM using a linker length of 7 amino acids. Rearrangement of the equation for K_d (eq 2a) and substituting the local concentration value for the free NarLN concentration [*N*] gives the closed [*CN*] to open NarLC [*C*] ratio. The ratio is 200:1 and 1200:1 for the longer and shorter linkers, respectively. By comparison, the closed-to-open ratio in the phosphorylated state is 2:1 to 12:1 with the same dependence as above on linker length.

DISCUSSION

Several response regulators, such as FixJ, CheB, and NarL, have an amino-terminal receiver domain in which the nonphosphorylated form is proposed to inhibit the activity of the attached effector domain by blocking access to the functional regions. Phosphorylation is thought to disrupt this interaction thereby activating the molecule. In FixJ, phosphorylation drives dimerization, which disrupts the inhibitory interdomain interactions (*20*, *21*). In the crystal structure of CheB, the receiver domain blocks the active site and is therefore proposed to inhibit activity by this interaction (*11*, *12*). In both structures of NarL, the domain interface is the same, and the putative DNA-binding residues are blocked (*1*, *8*). In addition, isolated NarLC can bind DNA to similar levels as the phosphorylated full-length protein (Gunsalus, unpublished data). In these three cases, it is apparent that one aspect of effector domain regulation is inhibition by the presence of the receiver domain and that this inhibition is relieved by phosphorylation of the receiver domain.

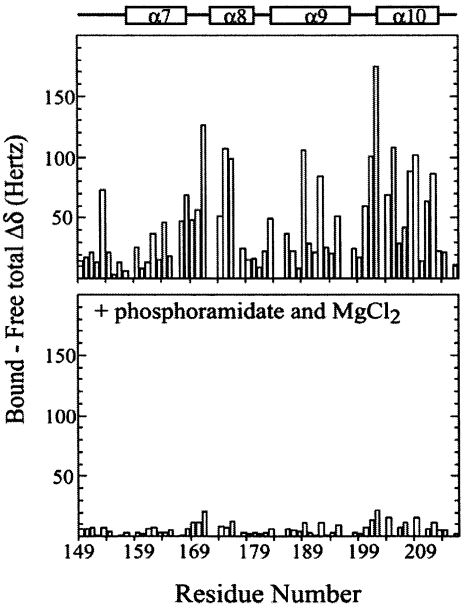

FIGURE 8: Comparison of the total chemical shift difference in NarLC as a function of residue number for the interaction of the two domains in buffer (top panel) and in buffer plus 120 mM phosphoramidate and 10 mM $MgCl_2$ (bottom panel).

The effect of phosphorylation on the structure of the receiver domain has been determined for several response regulators either in the phosphorylated state, NtrC (*22*), Spo0A (*23*), and FixJ (*21*), or in a state that mimics phosphorylation, phosphono-CheY (*24*) and BeF_3^--activated-CheY (*25*). Although the details of the phosphorylation-induced structural changes are unique to each molecule, there are some general trends. All of the proteins have structural changes in β4, α4, and the loop region between them. P-FixJ, BeF_3^--activated-CheY, and P-NtrC also have perturbations in the α3−β3 loop and in helix 3. Helix 5 is greatly affected in the two CheY analogues, and β5 is altered in P-NtrC. The overall effect of these changes is a localized change in the surface of the molecule. In the case of CheY, the altered regions contain part of the CheA, FliM, and CheZ binding sites (*25*, *26*). For NtrC, phosphorylation induces helix 4 to form a hydrophobic surface that is predicted to interact with another domain in the full-length protein (*22*). As mentioned above, phosphorylation drives dimerization in FixJ, which is proposed to disrupt the interdomain interface. The general effect of phosphorylation on receiver domain structure can be applied to other response regulators. In CheB, the region buried by the interdomain interface (α4−β5−α5) (*12*) corresponds well with the region altered by phosphorylation in the CheY analogues. This suggests a direct disruption of the interdomain interface upon phosphorylation. NarL has a

very different interdomain interface than CheB, and the possible mechanism of activation by phosphorylation is less clear. This study analyzed the interdomain interaction of NarL and the effect of phosphorylation on that interaction.

The interdomain interface of NarL was mapped by titrating the isolated domains and following the chemical shift changes of NarLC in the NMR. The chemical shift changes that occur in NarLC upon the addition of NarLN indicate that the domains interact in trans. Since only certain residues have altered chemical shifts, NarLC is not affected globally by the interaction with NarLN. Four lines of evidence indicate that the interaction is specific: (i) only particular residues are affected by the addition of NarLN; (ii) these residues are unaffected by the addition of a different response regulator, CheY; (iii) mapping the chemical shift changes onto the crystal structure indicates that many are in close proximity to residues in NarLN; and (iv) phosphorylation causes the NarLC peaks to nearly return to their unbound positions.

A comparison of the NarL crystal structures with the residues exhibiting large chemical shift changes predicts that these residues fall into two major classes. The first class includes those residues directly affected by the proximity of NarLN either because they are involved in an interaction with NarLN or because NarLN directly changes their chemical environment. The second class of residues are those internal to NarLC that are likely moving as a result of a conformational change. For example, residue 153 is distant from the interface but is in close proximity to another affected residue, 209. Residues not located at the interface may be important for stabilizing the active or inactive conformation. The residues most likely involved in the physical interaction between the domains are found in the loop region between helices 7 and 8, protruding down from helix 9, and certain residues in helix 10 (Figure 5). The residues in the first loop region, 170G and 171L, are in close proximity to the unique long loop region between helices 5 and 6 in NarLN. The carbonyl oxygen of 170G is predicted by MolMol (*9*) to form a hydrogen bond with the amide proton in residue 128M. Also, this glycine was proposed by Baikalov et al. (*1*) to be important for the correct orientation of helices 7 and 8. The orientation of these helices may be different in the free NarLC structure as there are several residues both in helix 7 and in helix 8 that have large chemical shift changes but do not appear close to any region of NarLN. Also, the long loop to helix 6 is not seen in any of the phosphorylation structures of the receiver domains, but the proximity to residues in NarLC suggests a role in maintaining the closed conformation.

Several other residues appear to be at the interaction site between the two domains. At the start of helix 8, the side chain of lysine 174 is predicted to be in a hydrogen bond with the first residue in the structure, glutamate 5. In helix 9, several residues have altered chemical shift, but only lysine 192 is near to a residue in NarLN, serine 80. Serine 80 is also predicted to form a hydrogen bond with the side chain of arginine 203. Serine 80 is in the $\alpha3-\beta4$ loop region, which was greatly affected by phosphorylation in the P-NtrC structure. Residues at the N-terminal end of helix 10 are near to the $\alpha4-\beta5$ loop region. The amide proton of residue 204 forms a putative hydrogen bond with the side chain oxygen of aspartate 104. Residues in the middle of helix 10 are in close proximity to the extra helix in NarLN, helix 6. Phosphorylation-dependent movement of helices 3 and 4 away from the active site could cause a clash with helix 6, disrupting the interaction with helix 10. Although there is no structure of the phosphorylated NarL, it is likely that it is similar to other response regulators. The regions of the receiver domain that could be responsible for disrupting the interface would therefore be helix 6 and the loops between $\alpha3-\beta4$, $\alpha4-\beta5$, and $\alpha5-\alpha6$. The first two loops have been shown for other receiver domains to be altered by phosphorylation, but the last long loop and helix 6 are novel to NarL. However, is not difficult to imagine how small perturbations could cause those regions to lose contact with the C-terminal domain.

Evidence that response regulators exist in equilibrium between active and nonactive conformations was found by Volkman et al. using the response regulator, NtrC (*27*). They showed that the residues experiencing motions on the microsecond time scale in the apo-protein are the same residues that undergo a large conformational change upon phosphorylation. These motions indicate exchange between at least two conformations of the protein, and the similarity to the phosphorylated form of the protein indicates that some active conformation exists in the nonphosphorylated protein. They postulated that phosphorylation shifts the equilibrium toward the active conformation.

It has been shown by bandshift assay that nonphosphorylated NarL can bind DNA at a reduced level and that NarLC alone can bind DNA at the same level as phosphorylated NarL (Gunsalus, unpublished results). This suggests that NarL, like NtrC, is in equilibrium between a conformation competent to bind DNA (open) and one in which the N-terminal receiver domain interferes with this process (closed). The observed dissociation constant between the domains in trans shows that the domains are not tightly bound. However, the relatively weak in trans binding is compensated by a large local concentration in the full-length molecule that results in a preponderance of the closed, as compared to the open conformation. Using two estimates of the local concentration, we estimate the open conformation to constitute between 0.1 and 1% of the NarL molecules. Phosphorylation decreases the affinity between the domains by 100-fold, thereby shifting the equilibrium toward the open conformation. However, even under phosphorylation conditions, we estimate that there could still be a preference for the bound or closed conformation in the full-length molecule.

The relationship between the interdomain interaction and DNA binding is proposed in Figure 9. In this model, the N-terminal domain occludes the DNA-binding residues of the C-terminal domain in the closed conformation, and only the open state can bind DNA. Our study indicates that, under normal conditions and in the absence of high concentrations of magnesium ion, the closed conformation is favored by approximately 200:1 (using the longest linker length). This preference is decreased 100-fold in the phosphorylated state. In the presence of 10 mM $MgCl_2$, the closed conformation is less favored but is still predominant at 50:1. If the intrinsic binding of DNA requires only the open state of the molecule, where $K_{int} = K'_{int}$, then a 25-fold excess of nonphosphorylated NarL in the presence of magnesium ion should bind DNA at the same level as phospho-NarL. However, it has been shown by DNAse protection that a 10-fold excess of

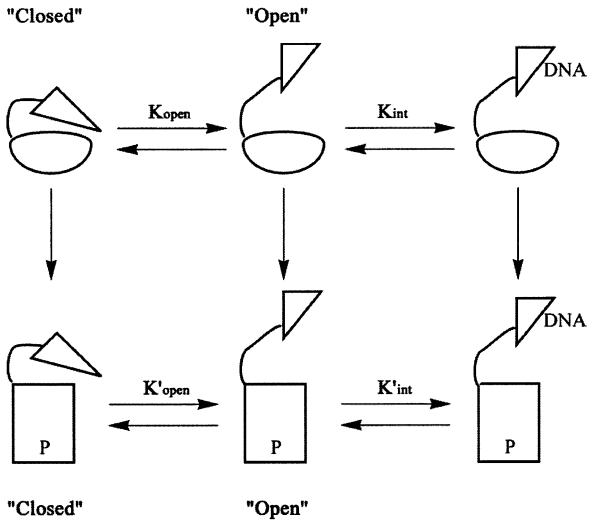

FIGURE 9: Six-state model for NarL activation and DNA binding. The equilibrium constant for NarL open and closed states is K_{open}, which is 1/200, assuming a 15-residue linker (see text). In the phosphorylated state the analogous K'_{open} is 1/2. The amount of DNA binding with respect to the open state is denoted by K_{int} and K'_{int} of the nonphosphorylated and phosphorylated states, respectively.

nonphosphorylated NarL can bind DNA about as well as phospho-NarL (Gunsalus, unpublished data). There are several potential explanations for this discrepancy. First, there is a possibility that the reaction conditions affect the apparent binding affinity. Perhaps differences in the small-molecule donors, buffers, or pH conditions play a role in the level of DNA binding or interdomain binding. There are other potential sources to account for the remaining discrepancy. There may be a low level of phospho-NarL in the DNAse assays, which would be undetectable by these methods. Also, the affinity of NarL for DNA may be stronger than in phospho-NarL so that $K_{int} \neq K'_{int}$. The linker may inhibit DNA binding in phospho-NarL or conversely aid DNA binding in the apo-protein. More experiments are needed to distinguish between these possibilities.

Our method of estimating local concentration assumes that the disordered residues not seen in the crystal structures are actually unfolded. This may not be the case. Thus, our estimates of the fractions of the molecule in the open and closed forms could be considerably different from the real ratio.

There are many questions still left unanswered for this system and for response regulators in general. Although we can show physical evidence of an interaction between the domains in the absence of a polypeptide linker and that this interaction is disrupted by phosphorylation, we do not know the mechanism of activation. For example, it is still possible that NarL behaves like FixJ, requiring dimerization for activation. The later structure of NarL predicted a dimer interface through helix 1, but no other evidence for such an interaction has been found (*28*). Also, it is known that NarL can bind to nontandem sites in the control regions of operons (*28*), suggesting that dimerization is not required for DNA binding.

ACKNOWLEDGMENT

We thank Megan McEvoy and Imke Schröder for their assistance in the early stages of this research. The work of A.M.E. was supported by a National Institutes of Health training grant GM007759.

REFERENCES

1. Baikalov, I., Schroder, I., Kaczor-Grzeskowiak, M., Grzeskowiak, K., Gunsalus, R. P., and Dickerson, R. E. (1996) *Biochemistry 35*, 11053−61.
2. Unden, G., and Bongaerts, J. (1997) *Biochim. Biophys. Acta 1320*, 217−34.
3. Gunsalus, R. P. (1992) *J. Bacteriol. 174*, 7069−74.
4. Stock, A. M., Robinson, V. L., and Goudreau, P. N. (2000) *Annu. Rev. Biochem. 69*, 183-215.
5. Stock, J., and Da Re, S. (2000) *Curr. Biol. 10*, R420−4.
6. West, A. H., and Stock, A. M. (2001) *Trends Biochem. Sci. 26*, 369−76.
7. Rabin, R. S., and Stewart, V. (1995) in *Two-Component Signal Transduction* (Silhavy, T. J., and Hoch, J. A., Eds.) pp 233−52, American Society for Microbiology, Washington, DC.
8. Baikalov, I., Schroder, I., Kaczor-Grzeskowiak, M., Cascio, D., Gunsalus, R. P., and Dickerson, R. E. (1998) *Biochemistry 37*, 3665−76.
9. Koradi, R., Billeter, M., and Wutrich, K. (1996) *J. Mol. Graphics 14*, 51−5.
10. Egan, S. M., and Stewart, V. (1991) *J. Bacteriol. 173*, 4424−32.
11. Anand, G. S., Goudreau, P. N., and Stock, A. M. (1998) *Biochemistry 37*, 14038−47.
12. Djordjevic, S., Goudreau, P. N., Xu, Q., Stock, A. M., and West, A. H. (1998) *Proc. Natl. Acad. Sci. U.S.A. 95*, 1381−6.
13. Ouwen Zhang, L. E. K., Olivier, J. P., and Forman-Kay, J. D. (1994) *J. Biomol. NMR 4*, 845−58.
14. Mueller, M. W. A. L. (1993) *J. Magn. Reson., Ser. B 101*, 201−5.
15. Grzesiek, S., and Bax, A. (1993) *J. Biomol. NMR 3*, 185−204.
16. Grzesiek, S., Anglister, J., and Bax, A. (1993) *J. Magn. Reson. Ser. B*, *101* 114−9.
17. Kim, S., Cullis, D. N., Feig, L. A., and Baleja, J. D. (2001) *Biochemistry 40*, 6776−85.
18. Schroder, I., Wolin, C. D., Cavicchioli, R., and Gunsalus, R. P. (1994) *J. Bacteriol. 176*, 4985−92.
19. Zhou, H. X. (2001) *Biochemistry 40*, 15069−73.
20. Da Re, S., Schumacher, J., Rousseau, P., Fourment, J., Ebel, C., and Kahn, D. (1999) *Mol. Microbiol. 34*, 504−11.
21. Birck, C., Mourey, L., Gouet, P., Fabry, B., Schumacher, J., Rousseau, P., Kahn, D., and Samama, J. P. (1999) *Struct. Fold Des. 7*, 1505−15.
22. Kern, D., Volkman, B. F., Luginbuhl, P., Nohaile, M. J., Kustu, S., and Wemmer, D. E. (1999) *Nature 402*, 894−8.
23. Lewis, R. J., Brannigan, J. A., Muchova, K., Barak, I., and Wilkinson, A. J. (1999) *J. Mol. Biol. 294*, 9−15.
24. Halkides, C. J., McEvoy, M. M., Casper, E., Matsumura, P., Volz, K., and Dahlquist, F. W. (2000) *Biochemistry 39*, 5280−6.
25. Lee, S. Y., Cho, H. S., Pelton, J. G., Yan, D., Berry, E. A., and Wemmer, D. E. (2001) *J. Biol. Chem. 276*, 16425−31.
26. McEvoy, M. M., Bren, A., Eisenbach, M., and Dahlquist, F. W. (1999) *J. Mol. Biol. 289*, 1423−33.
27. Volkman, B. F., Lipson, D., Wemmer, D. E., and Kern, D. (2001) *Science 291*, 2429−33.
28. Darwin, A. J., Tyson, K. L., Busby, S. J., and Stewart, V. (1997) *Mol. Microbiol. 25*, 583−95.

BI026254+